

A NUMERICAL STUDY OF MIXING AND STRATIFICATION DYNAMICS IN THE RIA DE AROUSA ESTUARY (NW SPAIN) DURING SUMMER

María Bermúdez¹, Julie D. Pietrzak², Luis Cea¹, Jerónimo Puertas¹, Guus S. Stelling^{2,3}, Gerben J. de Boer^{2,3}

Abstract

In this paper we explore the role of the river run-off, the tidal regime and the local winds in the dynamics of the Ria de Arousa estuary during the summer period, using for that purpose the numerical model Delft3D. First of all, a simulation under real hydrological and meteorological conditions is conducted in order to validate the ability of the model to reproduce measured salinity and temperature profiles. Subsequently, a series of simulations considering simplified meteorological input data and river discharge conditions are carried out in order to study the sensitivity of stratification conditions in the estuary to the various external forcings of the model. The results are analyzed using potential energy anomaly arguments, which allow quantifying and ranking the contribution of the different processes to the stratification of the estuarine system.

Key words: Ria de Arousa estuary, 3D numerical model, potential energy anomaly, mixing and stratification

1. Introduction

The Ria de Arousa is one of the four main embayments of the Rias Baixas region in NW Spain, located at approximately 42.5 °N with a SW-NE main channel alignment (Figure 1). The most important human activity in this area is that of edible mussel culture. The Rias Baixas produce annually more than 250,000 tons of mussels, which represent 25% of the world production, being the highest raft density found in the ria de Arousa. This high yield of mussel culture has been found to be a direct consequence of the seston characteristics in the ria, which in turn depend on water circulation in the adjacent shelf sea and inside the estuary (Figueiras et al., 2002).

The estuary is usually classified as a partially mixed estuary during the whole year. In winter, stratification is determined by the river freshwater input, while in summer it is caused by solar heating. Thus, in contrast with the classical definition of estuaries, forcing by continental runoff is not a key factor controlling the circulation pattern during the summer period (Alvarez-Salgado et al., 2000).

The main oceanographic process that occurs in this area is the succession of upwelling and downwelling events in accordance with the dominant shelf winds. Upwelling-favourable northerly winds prevail from March-April to September-October, while downwelling-favourable southerly winds dominate the rest of the year. However, 70% of the wind regime variability observed is concentrated in periods of less than 30 days (Alvarez-Salgado, 2003), and winds actually cycle between episodes favouring upwelling and downwelling during the “upwelling season”. Therefore, a short time-scale variability of the hydrographic and circulation structures can be observed, both on the shelf and inside the Rias.

Varela et al. (2005) reviewed the water masses existing in the Rias Baixas adjacent shelf region, as well as their circulation patterns. During upwelling episodes, the northerly winds exert a southward surface stress causing an Ekman transport offshore. The displaced surface water is replaced by the colder, nutrient-rich deeper water known as Eastern North Atlantic Central Water (ENACW), and the positive estuarine circulation is enhanced (Figure 1).

These upwelling events, together with the circulation patterns inside the estuary, govern the chemical

¹ Civil Engineering School, A Coruña University, Campus de Elviña, s/n, 15071 A Coruña, Spain. mbermudez@udc.es / lcea@udc.es / jpuertas@udc.es

² Section of Environmental Fluid Mechanics, Delft University of Technology, P.O. Box, 5048, NL-2600 GA, Delft, The Netherlands. j.d.pietrzak@tudelft.nl / g.s.stelling@tudelft.nl / g.j.deboer@tudelft.nl

³ Deltares, Delft, the Netherlands. guus.stelling@deltares.nl / gerben.deboer@deltares.nl

and biological properties of the water. The upwelled ENACW fertilizes the water column and controls the phytoplankton accumulation inside the ria (Roson et al., 1995). This is very relevant to mussel aquaculture management, since the phytoplankton concentration and the current velocity have been found to explain the 98% of the variance of the growth rates in length and dry weight of cultured mussels in the Rias Baixas (Perez-Camacho et al., 1995). For other biological implications of the upwelling phenomenon, which are beyond the scope of this paper, we refer to work published by Pitcher et al. (2010) or Varela et al. (2008).

A considerable amount of research has focused on the large-scale dynamics of these coastal inlets (Blanton et al., 1984; Prego and Fraga, 1992; Figueiras et al., 1994; Tilstone et al., 1994; Alvarez-Salgado et al., 1996, just to mention a few). The above studies emphasize the importance of the shelf wind stress and the Coriolis effect on the circulation and, consequently, on the thermohaline properties of the water at the mouth of the Rias.

On the contrary, the role of wind-driven currents inside the estuaries has received far less attention. Within the Rias, the wind in the shelf is channelled by the topography along the main axis, i.e., approximately in the NE-SW direction, either offshore or onshore directed (Herrera et al., 2005). In this short-scale, Coriolis force can be neglected due to the physical dimensions of the estuaries, and it is the ageostrophic response of the system which will increase or decrease the positive estuarine circulation (Figure 1).

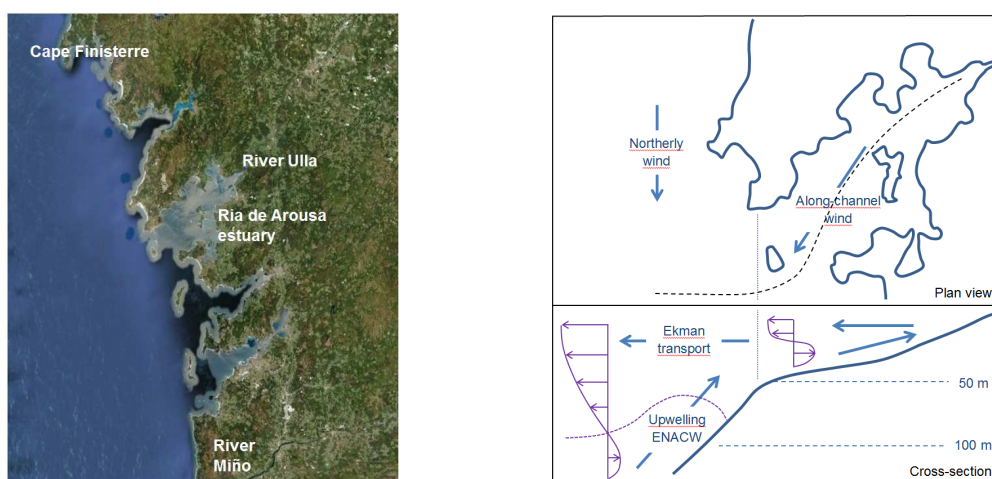


Figure 1. Location of the Ría de Arousa within the Galician Rías Baixas (left) and sketch of the wind-driven circulation in the study area (right). Large-scale Ekman response (outer part) and localized upwelling due to along-channel wind (inner part).

In this paper we explore the role of the river run-off, the tidal regime and the local winds in the dynamics of the Ria de Arousa during the summer period, by means of numerical modeling. Previous numerical studies in the Rias (Alvarez-Salgado et al., 2000 or Roson et al., 1997) have successfully employed a 2D non-steady-state, salinity-temperature weighted box model for calculating the residual fluxes. Nevertheless, due to the permanent stratification of the water column, a 3-dimensional model is required for a complete description of the flow. To the authors' best knowledge, previous works using this approach have either neglected wind forcing within the Rias (Taboada et al., 1998 or Montero et al., 1999 in the Ria de Vigo) or considered a rough estimation of local winds from shelf wind data (Souto et al., 2003 or Torres et al. 2001 also in the Ria de Vigo). Besides, no common methodology has been established to quantify the role of wind, tides and freshwater flows in the estuarine dynamics.

The aim of this paper is to gain a better understanding of the short-scale physical processes in the Ria de Arousa, with special attention to along-channel wind forcing. To this end, the flow module of Delft3D is used to conduct a simulation with real-data from summer 2010, in which meteorological input data are obtained from a weather station inside the ria. The results are compared with measured salinity and temperature profiles to evaluate the ability of the model to reproduce the observed features. Subsequently, a set of simulations with simplified boundary conditions and meteorological input data is carried out to determine the relative importance of wind forcing, freshwater buoyancy input and tidal forcing in the

estuarine circulation. The results are analyzed using the potential energy anomaly equation, derived as shown in de Boer et al. (2008), which allows quantifying and ranking the contribution of the different processes to the stratification of the estuarine system.

2. Methodology

2.1. Study site

Ria de Arousa is a partially mixed estuary on the west coast of Galicia (NW Spain, 42.5° latitude North) with a SW-NE orientation. The total surface of the estuary is approximately 239 km², with a length of 33 km and an average width of 9 km. The inner part of the estuary is less than 20 m deep, while in the outer area Salvora island divides the entrance into a narrow and shallow northern mouth (~10 m deep) and a wider and deeper southern mouth (50–60 m deep). Salvora island also protects the estuary from wave action.

Two main rivers flow into this estuary, the Ulla and the Umia, at a low discharge rate in the summer period (during June-September 2010 the average discharge was 24.9 m³/s and 4.2 m³/s, respectively). The tidal forcing is mainly semi-diurnal with M2 (amplitude of about 1.1 m) modulated over the spring-neaps cycle by S2 and N2 (of around 0.4 m and 0.2 m amplitude, respectively).

At different oceanographic stations within the estuary, temperature and salinity vertical profiles are measured with CTD (Conductivity-Temperature-Depth) profilers by the Technological Institute for Galicia's Marine Environment Control (INTECMAR), on a weekly basis since 2006. These data show how the stratification is generally weak in winter, particularly thermal stratification, while it increases during the summer period. In the outer area of the estuary, water temperature varies between 11 and 20 °C during summer. Due to the low river discharges, salinity differences between the top and bottom are generally below 1 ppt and the salinity is usually over 34 ppt, except in the innermost zone of the estuary. Therefore, density differences in this period are controlled by temperature rather than by salinity.

2.2. Numerical model

The numerical model used in this study is the hydrodynamic module of Delft3D, a complete description of which is available in Deltares (2012). Examples of successful applications of this model in coastal regions and estuaries can be found in De Boer et al. 2006, Kuang et al., 2011 or Twigt et al, 2009. The model solves the Reynolds averaged Navier Stokes equations under the shallow water and the Boussinesq assumptions, using sigma-coordinates. Spatial discretization is done in a structured grid. For the spatial discretization of the advection terms, a combination of a third-order upwind scheme in the horizontal direction and a second-order central scheme in the vertical is used (the Cyclic-method, Deltares, 2012). For time discretization, an alternate direction implicit scheme is employed.

The salinity and heat transport is modelled by an advection-diffusion equation in three coordinate direction, which is also solved using the so-called cyclic-method. For vertical mixing, the eddy viscosity is computed with the standard k-ε model. In the horizontal plane, constant values of eddy viscosity and diffusivity are applied.

The algorithm developed by Stelling and Van Kester (1994) to approximate the horizontal diffusion along Z-planes in a sigma-coordinate framework is applied in order to reduce the artificial vertical diffusion. In the vertical direction, the Forester filter (Forester, 1977) is also used to remove small non-physical oscillations introduced by the numerical scheme for the vertical advection of heat and salinity.

2.3. Model setup

The numerical computations are performed in a curvilinear boundary-fitted grid which contains 7424 computational elements in the horizontal plane and 25 equidistant sigma-layers in the vertical direction (Figure 2). The grid size is approximately 200 m in the inner part of the domain and increases progressively towards the sea boundary until it reaches 500 m in the outer part of the estuary. The model is run with a time step of 1 minute.

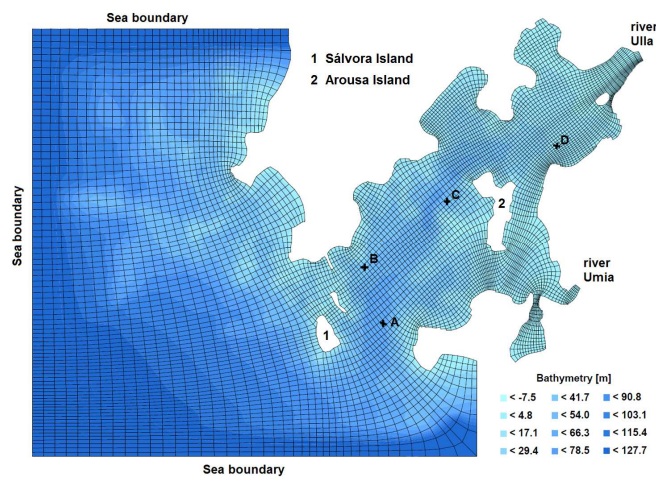


Figure 2. Bathymetry and curvilinear mesh of the Ria de Arousa (NW Spain) used in the numerical model. Location of control points (A-D) and open boundaries.

Regarding the physical parameters of the model, the bottom roughness is specified over the whole area with a constant Manning coefficient of $0.03 \text{ s/m}^{1/3}$. In the horizontal plane, a constant eddy viscosity and eddy diffusivity of $1 \text{ m}^2/\text{s}$ are applied. In the vertical direction, a background eddy viscosity of $10^{-4} \text{ m}^2/\text{s}$ is imposed and the standard k- ϵ model is selected. Wave induced mixing is neglected in the model, since the area is well protected from wave action.

The model is forced at the sea boundaries with the tidal harmonics extracted from the FES2004 solution (Lyard et al, 2006), a constant vertical salinity profile of 35.8 ppt and a weekly constant vertical temperature profile according to measurements from NOAA/OAR/ESRL PSD (Boulder, Colorado, USA) web site at www.esrl.noaa.gov/psd. At the river boundaries, measured daily discharge from Aguas de Galicia (2010) and daily temperature from Parada et al. (2011) are imposed. The solar radiation, air temperature, relative humidity, wind velocity and wind direction are imposed from measurements at time intervals of 10 min obtained from the meteorological station of Salvora (Figure 3) (www.meteogalicia.es). An average constant cloudiness of 20% is assumed during the whole period.

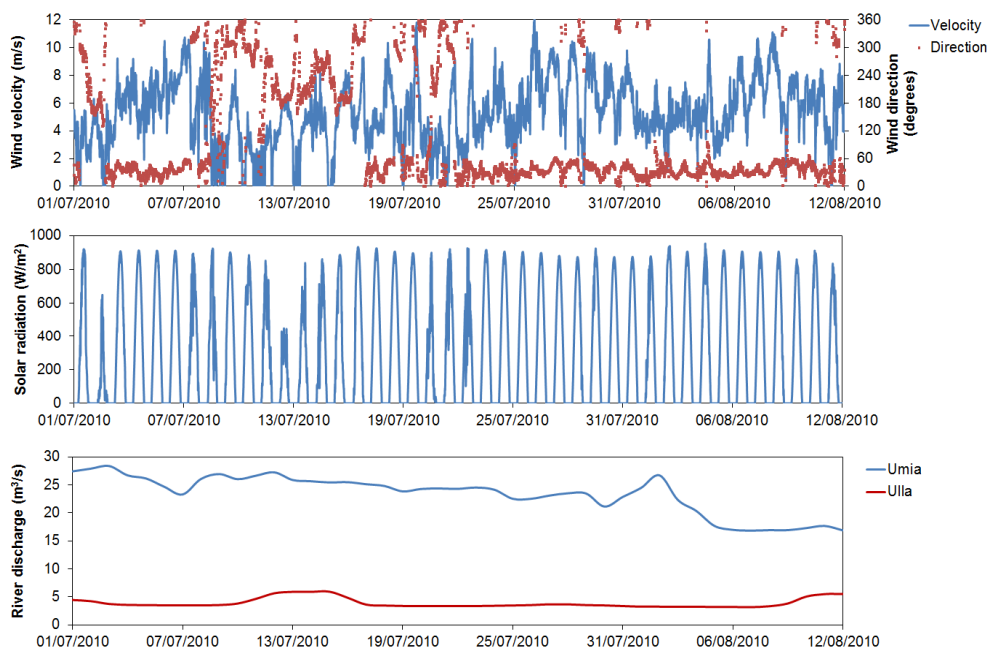


Figure 3. Wind velocity and direction, solar radiation and river discharges for the selected period.

The simulation covers the period from 1 July to 12 August 2010. A previous spin-up simulation of 60 tidal cycles, with average summer discharge and meteorological conditions, is used to initialize the simulation.

2.4. Potential energy anomaly equation

Previous studies in regions of freshwater influence or ROFIs (De Boer et al, 2008; Marques et al., 2010) have successfully employed potential energy arguments to evaluate the influence of the different physical mechanisms that control stratification and mixing. The potential energy anomaly ϕ , as given by Simpson and Bowers (1981), represents the depth-averaged amount of energy per unit volume required to obtain a fully mixed water column:

$$\phi = \frac{1}{H} \int_{-h}^{\eta} (\bar{\rho} - \rho) g z dz \quad \bar{\rho} = \frac{1}{H} \int_{-h}^{\eta} \rho dz \quad (1)$$

where H is the total depth of the water column, given by $H = \eta + h$, η is the free surface elevation, h is the location of the bed, ρ is the water density and g is the gravity acceleration.

In this study, two methods of analysis have been adopted. On the one hand, the potential energy anomaly ϕ is integrated over the study area to analyze mixing and straining of the system over time, as in previous work from Van Wiechen (2011). This study uses the same method, but it incorporates the realistic bathymetry and coastline of the Ria de Arousa. The spatially integrated potential energy anomaly E is defined as:

$$E = \iint \phi dAdz \quad (2)$$

where E represents the total amount of energy required for complete mixing.

The second method is based on the potential energy anomaly equation suitable for three-dimensional flows, derived as shown in de Boer et al. (2008). Previous studies report horizontal diffusion, source and sink and barotropic terms as negligible for controlling the changes in stratification of real systems (Burchard and Hofmeister, 2008; de Boer et al., 2008). Given that surface and bed density fluxes are zero, the potential energy anomaly equation can be written as follows:

$$\frac{\partial \phi}{\partial t} \approx \frac{g}{H} \int_{-h}^{\eta} \left(\underbrace{\tilde{u} \frac{\partial \tilde{\rho}}{\partial x}}_{S_x} + \underbrace{\tilde{u} \frac{\partial \tilde{\rho}}{\partial x}}_{A_x} + \underbrace{\tilde{u} \frac{\partial \tilde{\rho}}{\partial x}}_{N_x} - \underbrace{\frac{1}{H} \frac{\partial \tilde{u} \tilde{\rho} H}{\partial x}}_{C_x} + \underbrace{w \frac{\partial \rho}{\partial z}}_{W_z} + \dots \right. \\ \left. \underbrace{\tilde{v} \frac{\partial \tilde{\rho}}{\partial y}}_{S_y} + \underbrace{\tilde{v} \frac{\partial \tilde{\rho}}{\partial y}}_{A_y} + \underbrace{\tilde{v} \frac{\partial \tilde{\rho}}{\partial y}}_{N_y} - \underbrace{\frac{1}{H} \frac{\partial \tilde{v} \tilde{\rho} H}{\partial y}}_{C_y} + \underbrace{\frac{\partial \langle \rho' w' \rangle}{\partial z}}_{M_z} \right) dz \quad (3)$$

where t, x, y, z represent the time and position coordinates, respectively; u, v, w represent the velocity components; $\bar{\rho}, \bar{u}, \bar{v}$ are depth averaged values; $\tilde{\rho}, \tilde{u}, \tilde{v}$ are the deviations from the depth averaged values; H is the water depth and $\langle \rho' w' \rangle$ is the turbulent flux of mass in the z direction. A two letter symbol is assigned to each depth integrated term, for easy notational purposes. Thus, Equation (3) reduces to:

$$\phi_t \equiv \frac{\partial \phi}{\partial t} \approx \left(\begin{matrix} S_x + A_x + N_x + C_x + W_z \\ S_y + A_y + N_y + C_y + M_z \end{matrix} \right) \equiv RHS \quad (4)$$

where S_x and S_y represent the straining terms, A_x and A_y are the advection terms, N_x and N_y describe the non-linear interaction between the deviation of both density and velocity over their depth-averaged value, C_x and C_y describe the effect of velocity-density correlation over the vertical, M_z describes the effect of turbulent vertical mixing of the density profile, W_z is related to up and downwelling effects and the symbol RHS is used to denote all terms on the right hand side. For more details we refer to de Boer et al (2008) or

Burchard and Hofmeister (2008).

In this work, the covariance method is applied to the model output. The covariance between a term α of Equation (4) and φ_t is calculated as:

$$\begin{aligned} \text{cov}(\alpha, \varphi_t) &= \sum_{i=1}^N [(\alpha_i - \bar{\alpha})(\varphi_{t,i} - \bar{\varphi}_t)] \\ \bar{\alpha} &= \frac{1}{N} \sum_{i=1}^N \alpha_i \end{aligned} \quad (5)$$

where N is the number of time steps.

In order to conduct the potential energy anomaly analysis, a set of 9 numerical simulations of 10 days are performed using the same numerical parameters as in the summer 2010 modeling. Simplified boundary conditions and meteorological input data are adopted to facilitate the evaluation of the competing factors in mixing and stratification. Thus, the M2 tidal constituent, which is the largest in this location, serves as an average tide for use in the simulations. Regarding the heat flux model, constant values (corresponding to the average July 2010 conditions) are adopted for the relative humidity, air temperature and solar radiation. The condition of average tide combined with a 25 m³/s and 4 m³/s discharge in the rivers Ulla and Umia (average summer discharge in 2010), and in the absence of winds, is selected as the background reference case. In order to understand how the system responds to upwelling and downwelling favourable wind forcing, wind velocity magnitudes between 1.5 m/s and 5 m/s in NE and SW directions are tested. Similarly, both a twofold increase and a half reduction in the river discharges from the reference simulation are evaluated. The energy anomaly equation method is applied to the reference simulation output, considering a 10 days period and storing the results every 20 min.

3. Results and discussion

3.1. Performance of the model

In this section, the results from the summer 2010 simulation are presented and compared to the salinity and temperature profiles measured by the Technological Institute for Galicia's Marine Environment Control (INTECMAR). Figure 4 shows the comparison between the calculated and observed salinity and temperature profiles at four oceanographic stations shown in Figure 2 in two different periods (19th-20th of July and 10th-11th of August).

Firstly, the model is expected to reproduce the general characteristics of the summer period, i.e., the dominance of thermal stratification in comparison to haline stratification. This feature is correctly reproduced in the model. The salinity variation between bottom and surface is low compared to the temperature gradient. Besides, the model should reproduce the short-term variations on the vertical profiles caused by the interaction of the wind and the river discharges. Thus, during upwelling events the salinity levels are expected to increase while the temperature decreases due to the oceanic water entrance. On the contrary, during upwelling relaxation periods the entrance of oceanic water in the estuary diminishes, and the model should reflect a salinity drop and a temperature increase in the surface layer. Similarly, high river discharges should generate haline stratification, while low river discharges should smooth the vertical salinity profiles. The competition between all these processes is complex, and difficult to reproduce in the numerical model.

Another process which contributes to stratification and mixing is the tidal straining, which occurs on a shorter timescale than the processes described above. The model should also reproduce the variation of the water column structure over the semidiurnal tidal cycle. It should be pointed out that each profile in Figure 4 represents a different instant of time within the selected period and, accordingly, corresponds to a different tide level (Figure 4c, 4e and 4g correspond approximately to low tide, 4f and 4h to high tide and the rest to intermediate tide levels). No significant differences in the level of agreement between the observed and calculated profiles are detected as a function of the tide level.

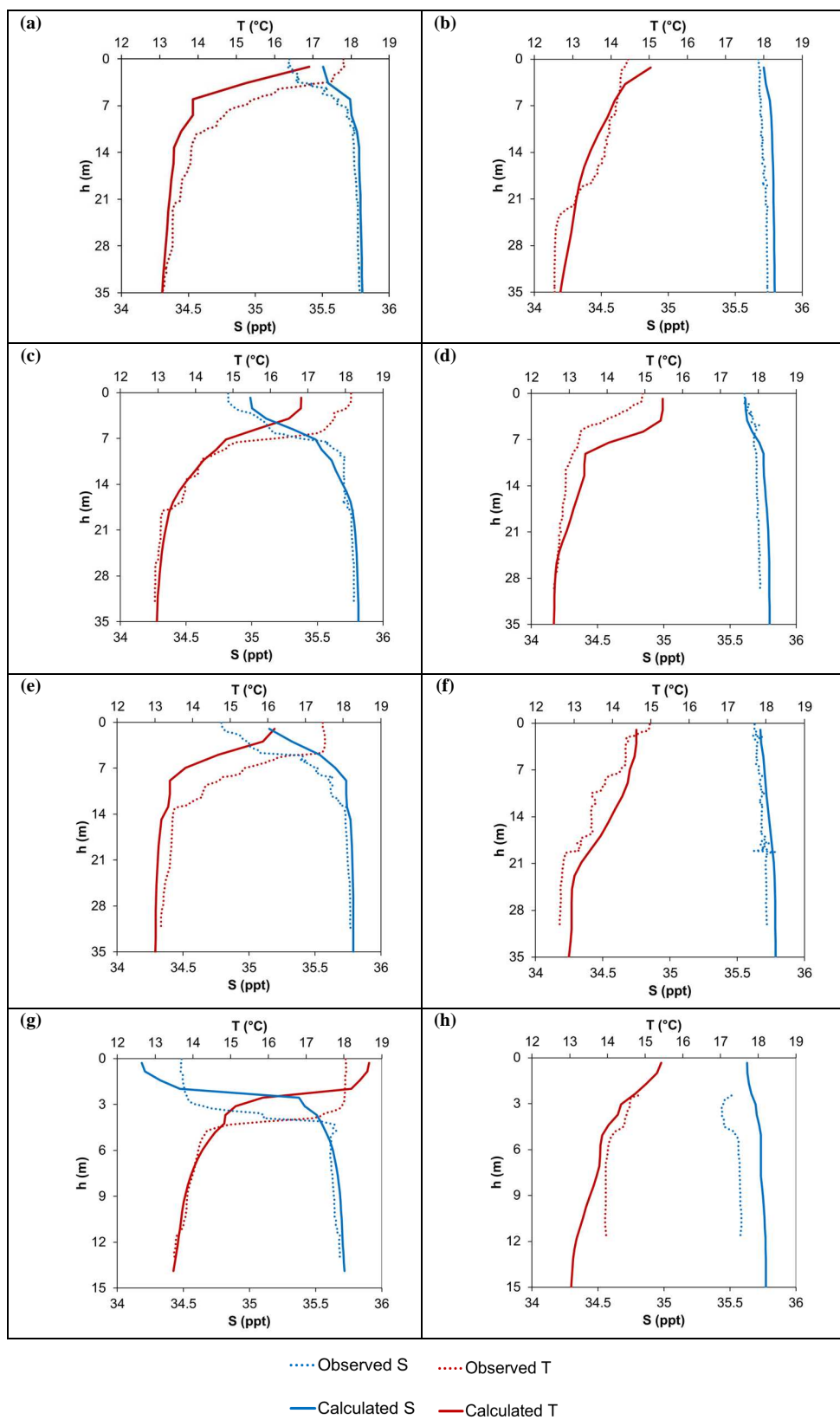


Figure 4. Vertical salinity (S) and temperature (T) profiles at control points A (a, b), B (c, d), C (e, f) and D (g, h) in the period 19th-20th July (left column) and in the period 10th-11th August (right column).

The first comparison period (19th-20th July 2010) is preceded by 10 days of south-westerly winds with an average velocity of 4 m/s and an average river discharge of 25.7 m³/s in the river Ulla and 4.6 m³/s in the river Umia. The observed profiles show a near-surface thermocline above 15 m depth, where the temperature increases approximately from 13°C to 18°C. In the first meters of the water column the salinity levels are also reduced slightly due to the freshwater river discharge. This decrease is more relevant in the inner part of the estuary (control point D), where it reaches 1.3 ppt. In this period, the agreement between the observed and calculated temperature and salinity profiles is satisfactory, as it can be seen in Figure 4. With the exception of point D, the surface temperatures predicted by the model are slightly lower than the observed ones (around 1°C). The salinity concentrations in the surface are underestimated, although the differences are below 0.5 ppt. Some differences in the position of the thermocline can also be reported, even though the general shape of the profiles is very similar.

During the preceding 19 days of the second comparison period (10th-11th August 2010), the wind was stronger (6 m/s on average) and NE becomes the predominant direction. The average river discharges are 21.4 m³/s and 3.5 m³/s for the river Ulla and Umia, respectively. In this period, higher salinity values are observed in the surface, which leads to an almost constant vertical salinity profile. On the other hand, surface temperature is around 15°C, which represents a difference of only 2°C with the bottom layers. As in the previous period, the results show a good fit between observed and simulated temperature and salinity values. However, small differences in the shape of the profiles can be noticed, especially at control points A and C, where the formation of a stepwise temperature distribution can be observed. Philips (1972) relates the formation of this structure to the instability of the density field due to the strong decrease of turbulent heat exchange coefficients with growing temperature gradients. For more details readers are referred to Barenblatt et al. (1993). Nevertheless, the model is able to capture the general trend of the profiles at all the control points.

Finally, the vertical eddy diffusivity profiles computed by the model are analysed, given the importance of correctly quantifying the vertical mixing rates (Figure 5). The vertical eddy diffusivity profiles deviate from the parabolic distribution which is frequently assumed to describe the vertical mixing in an open channel flow (Geyer, 1993). A region of small vertical eddy diffusivity D_v occurs within the thermocline, until 8 m depth on 20th July and extending up to 25 m depth on 11th August. The effects of wind and bottom shear stress can be seen in the upper and lower part of the profile, respectively. The eddy diffusivity is maximal close to the bottom, where the stratification is weakest.

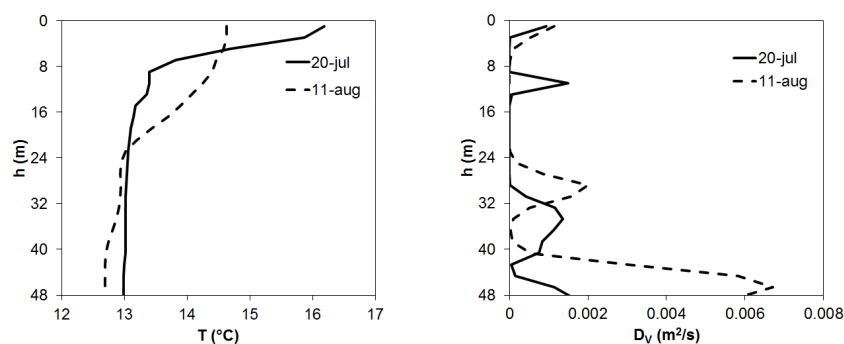


Figure 5. Temperature (T) and vertical eddy diffusivity (D_v) profiles computed by the model at control point C the 20th July, 06:10 h and the 11th August, 06:55h.

3.2. Potential energy anomaly analysis

3.2.1. Spatially integrated potential energy anomaly

The following discussion focuses on the response of the estuary to forcing by the wind and on the competition between the tide, the wind and the buoyancy input from the rivers Ulla and Umia. The potential energy anomaly is integrated over the whole domain for the 9 different scenarios described in section 2.4.

In the absence of wind, mixing and straining are controlled by the tide. The characteristic semi-diurnal oscillations in stability caused by the ebb-flood tidal cycle can be seen clearly in Figure 6. During ebb, warmer surface water is moved seaward faster than underlying cooler water and stratification is promoted. Thus, the energy required to mix the water column is maximal near low water (around 2.19 TJ). Conversely, during flood the bed shear counteracts the estuarine circulation to reduce stratification, and E reaches a minimum near high water (around 2.13 TJ). The fluctuations in stability within each tidal cycle can be considered small, since the variation of E is below 2.7%.

The second issue to be discussed is the impact of the magnitude and direction of the wind. Due to the limited computational domain considered in this study (Figure 2), the results refer to the local wind action. In Figure 6 the results of the integrated potential energy anomaly are plotted for different wind scenarios. With south-westerly winds, the energy required for full mixing follows a downward trend (Figure 6a). Accordingly, onshore wind appears to induce mixing of the water column and hence a reduction of stratification. The semidiurnal oscillations in energy E due to the tide continue to be perceived.

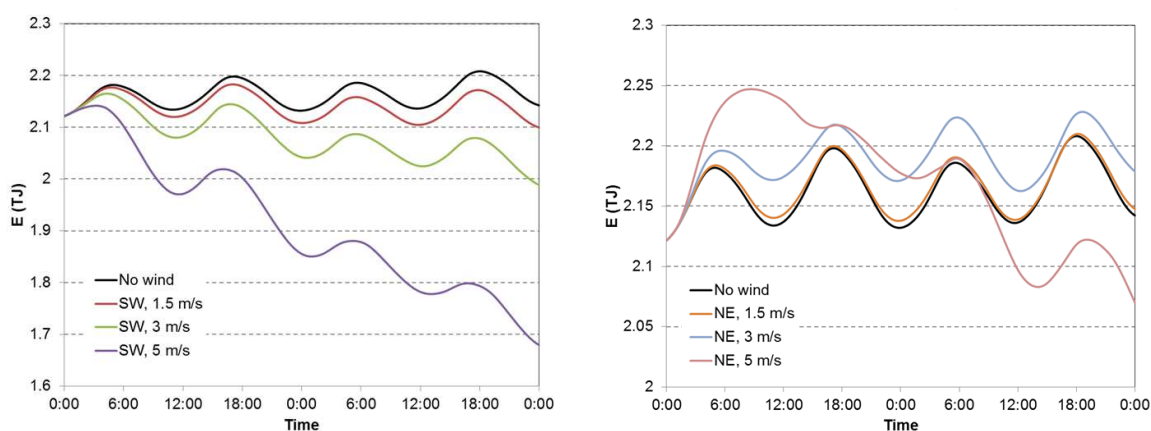


Figure 6. Evolution of the energy E required for complete mixing during 2 days under different wind conditions. Downwelling (left) and upwelling (right) favourable winds (SW and NE winds, respectively).

On the other hand, north-easterly winds can result in either an increase or decrease of stratification, depending on the wind magnitude. In the scenarios with lower wind speed (1.5 m/s and 3 m/s), higher values of energy E are obtained for the first two days of wind forcing (Figure 6b). Thus, moderate offshore wind seems to increase stratification, in spite of the mixing effect of the wind.

On the contrary, for the 5 m/s wind from the NE, the level of stratification decreases starting approximately from the second tidal cycle. Figure 7 shows the evolution of the energy E if the wind continues blowing for 10 days. It is observed that, from the second tidal cycle on, the amount of energy required to fully mix the Arousa estuary is clearly smaller than for the no-wind scenario. This suggests that, for this wind velocity, the vertical mixing generated by the wind overcomes the increase in stability due to upwelling advection. For the opposite wind direction (SW) and the same wind speed, the stirring effect of wind is added to the downwelling advection, which reduces even more the stratification. In both scenarios, the ebb-flood tidal cycle is visible in straining and mixing of the water column.

Finally, the role of buoyancy input from the riverine water is assessed, considering a twofold increase and a half reduction in the river discharges from the reference simulation. The time evolution of the energy E required for complete vertical mixing is very similar for both scenarios (Figure 7), the differences increasing progressively with time. Stratification becomes stronger for the high river inflow and weaker for the low freshwater discharge. Thus, the differences in energy E after 10 days are only around 5 %, reflecting a high response time of the estuarine density distribution to discharge variations within the studied range. It should also be noted that the stability fluctuations associated with the tide, i.e., the difference in E between high tide and low tide, increase slightly with the higher discharge.

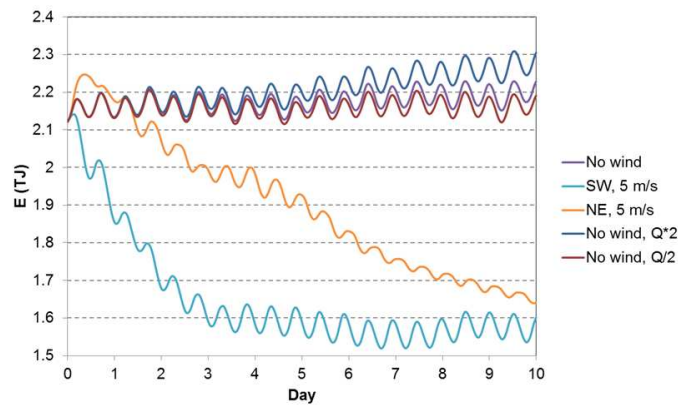


Figure 7. Evolution of the energy E required for complete mixing during 10 days, either with wind forcing or with a discharge variation with respect to the reference simulation.

3.2.2. Covariance analysis: spatial distribution of ϕ_t and ϕ_t predictors

The covariance between the individual terms in Equation (4) and the variation of the potential energy anomaly (ϕ_t) at each grid point in the model is presented in Figure 8. To compute the covariance, 20 tidal cycles sampled every 20 min were considered. The autovariance of ϕ_t (Fig8) is used to evaluate the magnitude of the variations in ϕ_t in the selected domain. The largest ϕ_t variations are located in the medium and outer part of the estuary, with the exception of the shallow areas near the Arousa Island. The covariance between the RHS and ϕ_t is practically identical to the autovariance of ϕ_t , indicating that RHS gives a good representation of ϕ_t .

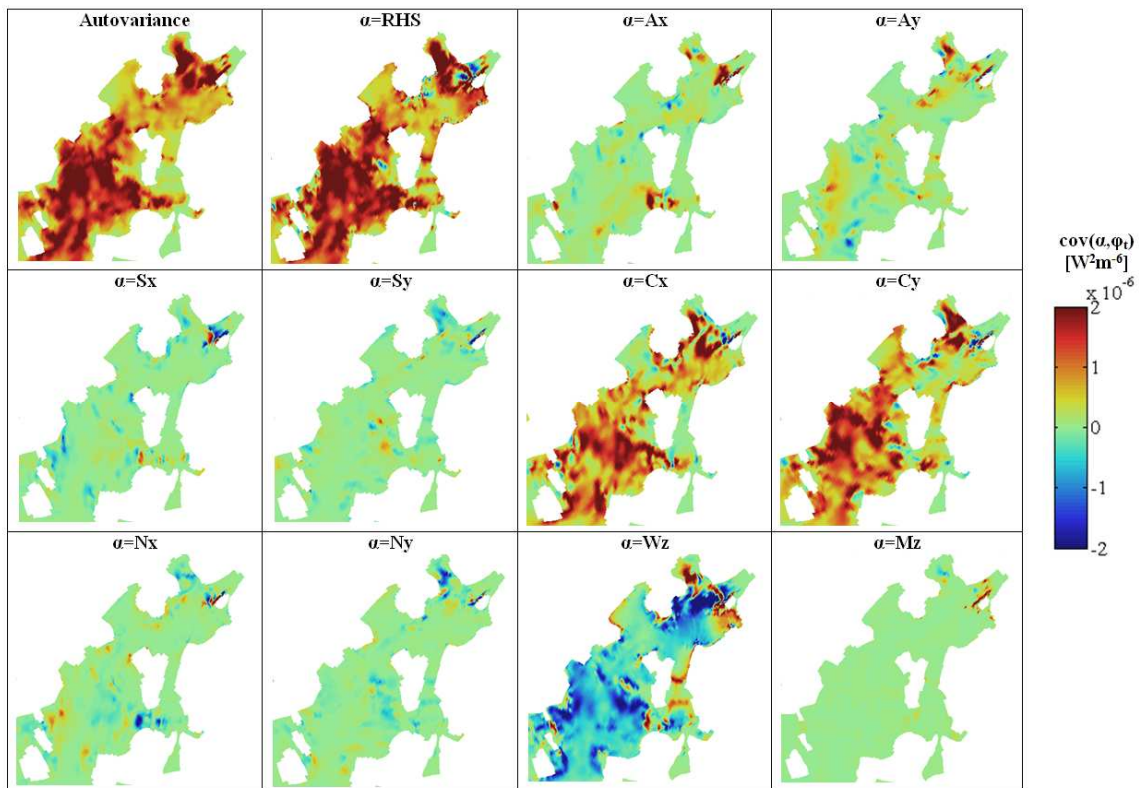


Figure 8. The covariance between the various terms in Equation (4) and ϕ_t as calculated from Equation (5). Autovariance of ϕ_t is proportional to the squared amplitude and RHS indicates the sum of the 10 terms in Equation (4).

The covariance is high in regions where the ϕ_t anomalies are important and the term under consideration is important to the maintenance of these anomalies, at the considered time scale. The results presented in Figure 8 show that both the dispersion terms (Cx and Cy) and the Wz term (related to up- and downwelling processes) play a significant role in the variation of the potential energy anomaly, followed by the advection terms (Ax and Ay). Cx, Cy and Wz exhibit a similar spatial pattern, and together with Ax and Ay almost describe the ϕ_t signal. The amplitude of the other terms (Sx, Sy, Nx and Ny) is much smaller.

4. Conclusions

The importance of the short-scale physical processes in the Ria de Arousa during the summer period was investigated through numerical modeling and the application of potential energy anomaly arguments. The numerical model results show a good fit with the observed temperature and salinity vertical profiles. The model seems to reproduce the general characteristics of the summer season, as well as the short-term variations on the vertical profiles observed in the selected period.

The analysis of the integrated potential energy anomaly time series reveals the important role of wind driven currents inside the estuary. Onshore wind appears to induce mixing of the water column and hence a reduction of stratification, the more pronounced the higher the wind speed. On the contrary, moderate offshore wind seems to increase stratification, in spite of the mixing effect of the wind. For both wind directions, the higher studied wind speeds reduce stratification. The other variations considered, including discharge variations within the summer range, appear to have much less impact on the estuarine dynamics.

The physical mechanisms controlling the stratification and mixing processes within the estuary were investigated through the application of the potential energy anomaly equation. The results suggest that the dispersion terms which represent the correlation between density and velocity over the vertical (Cx and Cy) and the up- and downwelling term (Wz) can serve as a simple explanation of the evolution of stratification in the estuary, for the time and spatial scale considered. On the other hand, turbulent diffusion, advection and straining seem to be much less relevant in the stratification processes.

Acknowledgements

The authors would like to thank the Spanish Ministry of Education (FPU grant reference AP2009-2070) and the Ministry of Science and Innovation (Ministerio de Ciencia e Innovación) for their financial support within the project 3D-MODEST (project reference CGL2011-28499-C03-03).

References

- Aguas de Galicia, 2010. Informe Anual 2009/2010 da Rede de Aforos de Galicia-Costa. Consellería de Medio Ambiente, Territorio e Infraestruturas. In Spanish.
- Álvarez-Salgado, X.A., Figueiras, F.G., Pérez, F.F., Groom, S., Nogueira, E., Borges, A.V., Chou, L., Castro, C.G., Moncoiffé, G., Ríos, A.F., Miller, A.E.J., Frankignoulle, M., Savidge, G., Wollast, R., 2003. The Portugal coastal counter current off NW Spain: new insights on its biogeochemical variability. *Progress in Oceanography*, 56: 281–321
- Álvarez-Salgado, X.A., Gago, J., Míguez, B.M., Gilcoto, M., Pérez, F.F., 2000. Surface Waters of the NW Iberian Margin: Upwelling on the Shelf versus Outwelling of Upwelled Waters from the Rías Baixas. *Estuarine, Coastal and Shelf Science*, 51(6): 821-837
- Alvarez-Salgado, X. A., Roson, G., Pérez, F.F., Figueiras, F.G., Pazos, Y., 1996. Nitrogen cycling in an estuarine upwelling system, the Ria de Arousa (NW Spain). I. Short-time-scale patterns of hydrodynamic and biogeochemical circulation. *Marine Ecology Progress Series* 135: 259-273
- Barenblatt et al. (1993)
- Blanton, J. O., Atkinson, L. P., Fernández, F., Lavín, A., 1984. Coastal upwelling off the Rias Bajas, Galicia, Northwest Spain, I: Hydrography studies. *Rapports et Proc-verbeaux Reun. Cons. Int. Explor. Mer*, 183, 79-90.
- Buchard, H., Hofmeister, R., 2008. A dynamic equation for the potential energy anomaly for analyzing mixing and stratification in estuaries and coastal seas. *Estuarine, Coastal and Shelf Science*, 77(4): 679-687.
- De Boer, G.J., Pietrzak, J.D., Winterwerp, J.C., 2008. Using the potential energy anomaly equation to investigate tidal straining and advection of stratification in a region of freshwater influence. *Ocean Modelling*, 22: 1-11
- De Boer, G.J., Pietrzak, J.D., Winterwerp, J.C., 2006. On the vertical structure of the Rhine region of freshwater influence. *Ocean Dynamics*, 56(3-4): 198-216.

- Deltares, 2012. Delft3D-FLOW user manual. Deltares, Delft (available via oss.deltares.nl).
- Figueiras, F.G., Labarta, U., Fernández Reiriz, M.J., 2002. Coastal upwelling, primary production and mussel growth in the Rías Baixas of Galicia. *Hydrobiologia*, 484: 121–131
- Figueiras, F. G., Jones, K. J., Mosquera, A. M., Álvarez-Salgado, X. A., Edwards, A., Macdougall, N., 1994. Red tide assemblage formation in an estuarine upwelling ecosystem: Ría de Vigo. *Journal of Plankton Research*, 16(7): 857–878.
- Forester, C. K., 1977. Higher Order Monotonic Convective Difference Schemes. *Journal of Computational Physics*, 23: 1–22.
- Herrera, J.L., Piedracoba, S., Varela, R.A., Rosón, G., 2005. Spatial analysis of the wind field on the western coast of Galicia (NW Spain) from in situ measurements. *Continental Shelf Research* 25(14): 1728–1748.
- Kuang, C., Lee, J.H.W., Harrison, P.J., Yin, K., 2011. Effect of wind speed and direction on summer tidal circulation and vertical mixing in Hong-Kong waters. *Journal of Coastal Research*, 27(6A): 74–86.
- Lyard, F., Lefevre, F., Letellier, T., Francis, O., 2006. Modelling the global ocean tides: modern insights from FES2004. *Ocean Dynamics*, 56(5-6): 394–415.
- Marques, W.C., Fernandes, E.H.L., Moller, O.O., 2010. Straining and advection contributions to the mixing process of the Patos Lagoon coastal plume, Brazil. *Journal of Geophysical Research*, 115, C06019.
- Montero, P., Gómez-Gesteira, M., Taboada, J.J., Ruiz-Villarreal, M., Santos, A.P., Neves, R.R., Prego, R., Pérez-Villar, V., 1999. On residual circulation of the Ria of Vigo, using a 3-D baroclinic model. *Bol. Inst. Esp. Oceanogr.*, 15(1-4): 31–38.
- Parada, J.M., Miranda, M., Martínez, G., Carreira, P., Molares, J., 2011. Temperatura y salinidad en los bancos marisqueros de Placeres, Sarrido, Bohído y Lombos do Ulla entre 2006 y 2010. Rías de Pontevedra y Arousa. Galicia. *Revista Galega dos Recursos Mariños (Datos)*: 2, 201 pp. In Spanish.
- Pérez-Camacho, A., Labarta, U., Beiras, R., 1995. Growth of mussels (*Mytilus edulis galloprovincialis*) on cultivation rafts: influence of seed source, cultivation site and phytoplankton availability. *Aquaculture* 138(1-4): 349–362.
- Pitcher, G.C., Figueiras, F.G., Hickey, B.M., Moita, M.T., 2010. The physical oceanography of upwelling systems and the development of harmful algal blooms. *Progress in Oceanography*, 55(1-2): 5–32.
- Prego, R., Fraga, F., 1992. A Simple Model to Calculate the Residual Flows in a Spanish Ria. *Hydrographic Consequences in the ria of Vigo. Estuarine, Coastal and Shelf Science*, 34(6): 603–615
- Rosón, G., Alvarez-Salgado, A., Pérez, F.F., 1997. A Non-stationary Box Model to Determine Residual Fluxes in a Partially Mixed Estuary, Based on Both Thermohaline Properties: Application to the Ria de Arousa (NW Spain). *Estuarine, Coastal and Shelf Science*, 44 (3): 249–262.
- Rosón, G., Pérez, F.F., Álvarez-Salgado, X.A., Figueiras, F.G., 1995. Variation of both thermohaline and chemical properties in an estuarine upwelling ecosystem: Ría de Arousa; I. Time evolution. *Estuarine, Coastal and Shelf Science*, 41(2): 195–213.
- Simpson, J.H., Bowers, D., 1981. Models of stratification and frontal movement in shelf seas. *Deep Sea Research*, 28A (7), 727–728.
- Souto, C., Gilcoto, M., Fariña-Busto, L., Pérez, F.F., 2003. Modeling the residual circulation of a coastal embayment affected by wind-driven upwelling: Circulation of the Ría de Vigo (NW Spain). *Journal of Geophysical Research*, 108 (C11), 3340.
- Stelling, G.S. Van Kester, J.A.T.M., 1994. On the approximation of horizontal gradients in sigma coordinates for bathymetry with steep bottom slopes. *International Journal for Numerical Methods in Fluids*, 18(10): 915–955.
- Taboada, J. J., Prego, R., Ruiz-Villarreal, M., Gomez-Gesteira, M., Montero, P., Santos, A.P., Perez-Villar, V., 1998. Evaluation of the seasonal variations in the residual circulation in the Ria of Vigo (NW Spain) by means of a 3D baroclinic model. *Estuarine, Coastal and Shelf Science*, 47(5): 661–670.
- Tilstone, G. H., Figueiras, F. G., Fraga, F., 1994. Upwelling-downwelling sequences in the generation of red tides in a coastal upwelling system. *Marine Ecology Progress Series*, 112: 241–253
- Torres, S., Varela, R. A., Delhez, E., 2001. Residual circulation and thermohaline distribution of the Ría de Vigo: A 3-D hydrodynamical model. *Scientia Marina*, 65(1): 277–289.
- Twigt, D.J., De Goede, E.D., Zijl, F., Schwanenberg, D., Chiu, A.Y.W., 2009. Coupled 1D-3D hydrodynamic modeling, with application to the Pearl River Delta. *Ocean Dynamics*, 59(6): 1077–1093.
- Van Wiechen, J., 2011. Modelling the wind-driven motions in the Rhine ROFI. MSc. Thesis, Delft University of Technology, Department of Civil Engineering and Geosciences.
- Varela, R., Roson, G., Herrera, J., Torres Lopez, S. and Fernandez Romero, A., 2005. A general view of the hydrographic and dynamical patterns of the Rías Baixas adjacent sea area. *Journal of Marine Systems*, 54(1-4): 97–113
- Varela, M., Prego, R., Pazos, Y., 2008. Spatial and temporal variability of phytoplankton biomass, primary production and community structure in the Pontevedra Ria (NW Iberian Peninsula): oceanographic periods and possible response to environmental changes. *Marine Biology* 154(3): 483–499.